Detection and quantification of structural damage under ambient vibration environment

Gun Jin Yun*

Department of Civil Engineering, The University of Akron, Akron, OH, 44325-3905, USA

Abstract. In this paper, a new damage detection and quantification method has been presented to perform detection and quantification of structural damage under ambient vibration loadings. To extract modal properties of the structural system under ambient excitation, natural excitation technique (NExT) and eigensystem realization algorithm (ERA) are employed. Sensitivity matrices of the dynamic residual force vector have been derived and used in the parameter subset selection method to identify multiple damaged locations. In the sequel, the steady state genetic algorithm (SSGA) is used to determine quantified levels of the identified damage by minimizing errors in the modal flexibility matrix. In this study, performance of the proposed damage detection and quantification methodology is evaluated using a finite element model of a truss structure with considerations of possible experimental errors and noises. A series of numerical examples with five different damage scenarios including a challengingly small damage level demonstrates that the proposed methodology can efficaciously detect and quantify damage under noisy ambient vibrations.

Keywords: modal identification; Eigensystem Realization Algorithm (ERA); Natural Excitation Technique (NExT); subset selection; genetic algorithm; damage detection; structural health monitoring

1. Introduction

Monitoring of structural integrity during service periods has increasingly become common not only for securing the safety of infrastructure, but also for minimizing maintenance costs. Recent developments of vibration-based structural health monitoring (SHM) techniques and current technological gaps can be found in numerous studies cited in the reference section of this paper (Beck *et al.* 1994, Doebling *et al.* 1998, Stubbs *et al.* 2000, Sohn *et al.* 2003, Caicedo *et al.* 2004, Lynch *et al.* 2004, Gao *et al.* 2006, Nayeri *et al.* 2007, Nayeri *et al.* 2008). Rationale of the vibration-based monitoring techniques is that modal properties (i.e., natural frequencies, mode shapes and modal damping ratios) are theoretically linked to structural changes. According to literatures (Friswell *et al.* 1997), natural frequencies could be insensitive to local and small damages in the structure. Therefore, substantial efforts have been put in development of robust and accurate techniques for monitoring and detecting damage.

Compared to the forced vibration test, ambient vibrations such as traffic-, wind- and pedestrian-

*Corresponding author, Assistant Professor, E-mail: gy3@uakron.edu

induced vibrations can be measured at any time during operations without operational interference or the use of special equipment for the excitation. By employing modal identification techniques such as eigensystem realization algorithm (ERA) technique (Juang *et al.* 1985), Ibrahim time domain (ITD) method (Ibrahim *et al.* 1977) and stochastic subspace iteration (SSI) technique (Van Overschee *et al.* 1996), *in-situ* measurements of the ambient vibration data have been successfully used for tracking structural changes of real-life buildings, bridges, and historical monuments caused by deterioration, damage, temperature, and any operational anomalies (Peeters *et al.* 2001, Wong 2004, Amani *et al.* 2007, Lee *et al.* 2007, Nayeri *et al.* 2007, Bani-Hani *et al.* 2008, Nayeri *et al.* 2008); the *in-situ* measurements have also been successfully used for building baseline finite element models for structural damage detection, condition assessment, and long-term SHM purposes (Farrar *et al.* 1997, Ren *et al.* 2005, Siringoringo *et al.* 2006, Duan *et al.* 2007, Gentile *et al.* 2008). In 2001, Bernal developed the damage locating vector (DLV) method, which has gained considerable attentions recently (Bernal 2002, Sim *et al.* 2008). Salient advantage of the DLV method is that the DLV vector can be computed strictly from measured data without the need to refer to any mathematical model. The DLV method is based on the principle of minimum potential energy and flexibility matrix. Friswell *et al.* suggested a subset selection method for use in locating damage; their method uses eigen-sensitivities, measuring the differences in natural frequencies between the damaged and undamaged states of a structure (Friswell *et al.* 1997). Yun *et al.* suggested a new parameter subset selection method based on sensitivity of dynamic residual force instead of simple sensitivity of natural frequencies and mode shapes; this method is known to be more accurate in identifying multiple damage locations than the original method (Yun *et al.* 2008, Yun *et al.* 2008). The subset selection method is fundamentally different from the DLV method in the fact that the subset selection method exploits a sensitivity matrix of a residual function of modal properties between simulations and experiments. The new subset selection method has not been demonstrated for the ambient vibration-based damage diagnosis.

For damage quantification, optimization problems are often formulated using cost functions in terms of modal properties. Most of the methods are categorized into two different methods: 1) heuristic optimization algorithm-based parameter search methods, and 2) gradient based numerical optimization methods. Genetic algorithms have been known to be robust in searching for global minimum or maximum values of cost functions; however, they have limitations due to the enormous computational times when using large-scale identification models. On the contrary, the gradient based searching methods can have difficulties in finding global minimum or maximum values when the initial solution is far different from the true solution. In particular, the steady state genetic algorithm is known to be faster than other standard or simple genetic algorithm methods without sacrificing its global searching capabilities (Syswerda 1991). There is a broad spectrum of vibration based damage diagnosis methods that adopt different techniques for damage detection, quantification, and consideration of uncertainties.

This paper proposes a new methodology for detecting and quantifying structural damage under ambient vibration, which combines the new parameter subset selection based damage detection with an evolutionary quantification method. Modal properties are identified by using NExT/ERA method. The proposed methodology consists of four major steps: 1) measurement of ambient vibration response; 2) modal identification using a time-domain output-only technique, NExT/ERA; 3) damage localization using a new parameter subset selection method; 4) damage quantification using a steady state genetic algorithm. A flowchart for the proposed methodology is illustrated in Fig. 1. Simulated ambient vibration testing of a truss bridge structure was conducted considering noise
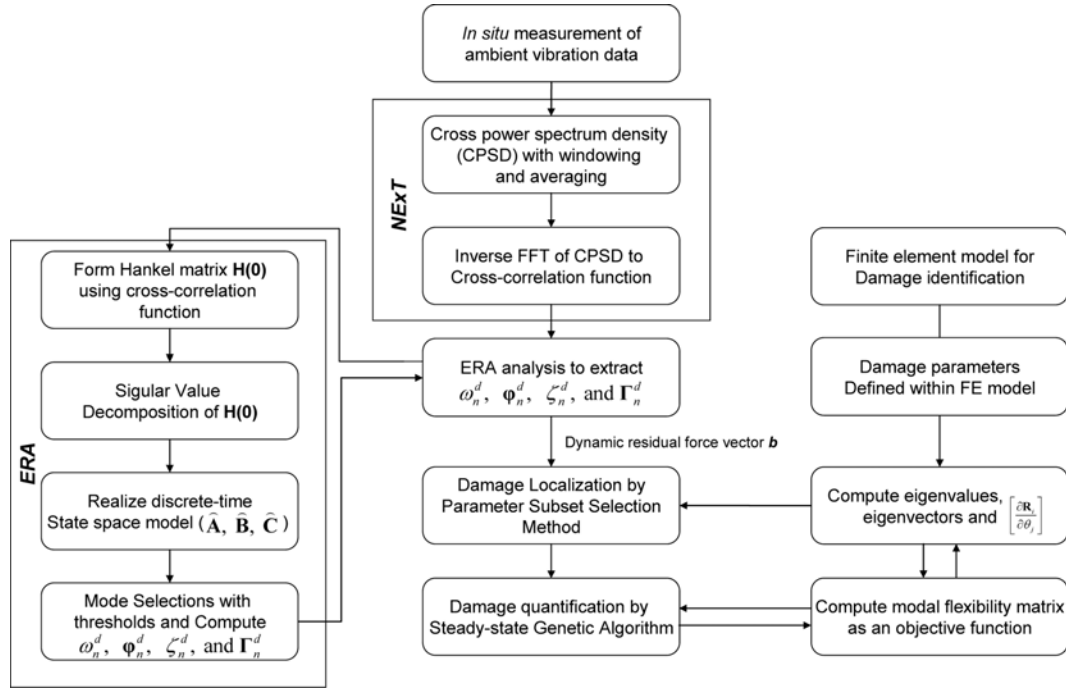
Fig. 1 A flow chart of the proposed ambient vibration based damage detection and quantification method

effects. A series of numerical examples with five different damage scenarios have been conducted under ambient vibration. Finally, the proposed methodology is proven to be efficacious in damage diagnosis and can potentially be applied to condition assessment of in-field structures.

2. Modal identification by NExT/ERA technique

2.1 Impulse Response by Natural Excitation Technique (NExT)

The theoretical justification of the NExT technique is based on the observation that correlation functions (auto- and cross-correlation functions) calculated from measured output data (commonly acceleration measurements) can be expressed in terms of sum of decaying sinusoids, which have the same damped natural frequency and damping ratio as the impulse response function of the original structural system. NExT is based on the two assumptions: 1) input excitations are a stationary random white noise and are uncorrelated with the response, which is also a weakly stationary random process, and 2) the structural system is excited within the linear elastic regime so that the principle of superposition is valid. In this section, the theoretical aspects will be revisited (James *et al.* 1993, Farrar *et al.* 1997). However, it is noteworthy that the first assumption is not necessarily satisfied, since the technique has been well applied to wind-, traffic- and pedestrian-induced ambient vibrations – which are not a completely random form of white noise. Solutions of the equation of motion decomposed in modal space are obtained using the Duhamel integral (or convolution integral). The response at ith degree of freedom (DOF) due to force $p_k(\tau)$ at kth DOF is expressed as

$$u_{ik}(t) = \sum_{r=1}^{n} \phi_i^r \phi_k^r \int_{-\infty}^{t} p_k(\tau) h^r(t-\tau)d\tau \tag{1}$$

where $h^r(t) = (1/(m^r \omega_D{}^r))\exp(-\zeta^r \omega_n{}^r t)\sin(\omega_D{}^r t)$ is the unit impulse response function corresponding to rth mode; n indicates the number of modes; and ϕ_i^r and ϕ_k^r are the ith and kth components of the rth mode shape. $\omega_D{}^r$ indicates the damped natural frequency of the rth mode, which is equal to $\omega_n{}^r (1 - \zeta^{r2})^{-1/2}$. To calculate the impulse response function, $p_k(t)$ is assumed to be a Dirac delta function at $\tau = 0$. The integration is then dropped in Eq. (1), which is expressed as

$$u_{ik}(t) = \sum_{r=1}^{n} \frac{\phi_i^r \phi_k^r}{m^r \omega_D^r} e^{(-\zeta^r \omega_n^i t)} \sin(\omega_D^r t) \tag{2}$$

The key idea of the NExT technique is the similarity between the cross-correlation function (Eq. (3)) and the impulse response function in Eq. (2) in terms of damped natural frequency and damping ratio. Assuming that system response is a stationary random process, the cross-correlation functions between two outputs at points i and j are defined as (Bendat *et al.* 2000)

$$R_{ijk}(S) = E[u_{ik}(t)u_{jk}(t+S)] \tag{3}$$

where $E[\ ]$ indicates the expectation operator. By substituting Eq. (1) into Eq. (3) and simplifying further, based on an assumption that input excitation is a white noise randomprocess, the correlation functions can be expressed as follows

$$R_{ijk}(S) = \sum_{r=1}^{n}\sum_{s=1}^{n} \phi_i^r \phi_k^r \phi_j^s \phi_k^s \int_{0}^{\infty} h^r(\lambda) h^s(\lambda+S)d\lambda \tag{4}$$

Further algebraic manipulation and simplification allows Eq. (4) to be in a form that has the same modal characteristics as the impulse response of original system, i.e., Eq. (2). Thus, the correlation function calculated from the displacement response at two points satisfies the homogeneous equation of motion. By Wiener-Khintchine relations, the cross-correlation functions and the cross-power spectral density (CPSD) functions form a Fourier transform pair as follows

$$R_{\ddot{u}_a \ddot{u}_b}(\tau) = \int_{-\infty}^{+\infty} R_{\ddot{u}_a \ddot{u}_b}(\omega) e^{j\omega\tau} d\omega \tag{5}$$

where $R_{\ddot{u}_a \ddot{u}_b}(\omega)$ indicates the CPSD function. Thus, the cross-power spectral density is first calculated using a built-in MATLAB function (*cpsd.m*) and then it is transformed to a correlation function through discrete inverse Fourier transform using a built-in MATLAB function (*ifft.m*). To improve signals by reducing non-reproducible noise, ensemble averaging and windowing techniques are employed. Once the impulse response of the system is obtained, ERA is used for modal identification, as discussed in the following section.

2.2 Modal Identification by Eigensystem Realization Analysis (ERA)

In this section, the Eigensystem realization analysis (ERA) is briefly introduced. Details on the derivation can be found in (Juang *et al.* 1985, Juang 1994). The ERA is originally based on Ho-

Kalman procedure for realization of the space-state model of linear systems (Ho *et al.* 1965). A finite-dimensional linear time-invariant system can be written in a state-space form as follows

$$\dot{\mathbf{x}} = \mathbf{A}_c\mathbf{x} + \mathbf{B}_c\mathbf{p} \qquad \mathbf{x}(k+1) = \mathbf{A}\mathbf{x}(k) + \mathbf{B}\mathbf{p}(k)$$

$$\mathbf{y} = \mathbf{C}_c\mathbf{x} + \mathbf{D}_c\mathbf{p} \qquad \mathbf{y}(k) = \mathbf{C}\mathbf{x}(k) + \mathbf{D}\mathbf{p}(k) \tag{6}$$

where $\mathbf{x}$, $\mathbf{p}$, and $\mathbf{y}$ are the state ($n \times 1$), control or input ($r \times 1$) and output vector ($m \times 1$), respectively. $\mathbf{A}_c$, $\mathbf{B}_c$, $\mathbf{C}_c$ and $\mathbf{D}_c$ are constant matrices representing a continuous-time system and $\mathbf{A}$, $\mathbf{B}$, $\mathbf{C}$ and $\mathbf{D}$ are for a discrete-time system. Considering the impulse response of the system under zero-initial condition ($u_i(0) = 1$ for $i = 1, 2,\ldots, r$ and $u_i(k) = 0$ for $i = 1, 2,\ldots, r$), the system Markov parameter can be obtained as

$$\mathbf{Y}_k = \mathbf{y}(k) = \mathbf{C}e^{\mathbf{A}_c(k-1)\Delta t}\mathbf{B} = \mathbf{C}\mathbf{A}^{k-1}\mathbf{B} \tag{7}$$

where $\mathbf{Y}_k$ indicates the system Markov parameter matrix having a dimension ($m \times r$) and $\mathbf{A}$ indicates the system matrix in discrete-time representation. The primary objective of the ERA analysis is to reconstruct the discrete-time model identified by a triplet [$\mathbf{A}$, $\mathbf{B}$, and $\mathbf{C}$] from the impulse response. Since $\mathbf{D} = \mathbf{Y}_0$, only the triplet needs to be reconstructed. ERA starts with the construction of a Hankel matrix, which consists of pulse response samples.

$$\mathbf{H}(k-1) = \mathbf{P}_\alpha\mathbf{A}^{k-1}\mathbf{Q}_\beta; \quad \mathbf{H}(0) = \begin{bmatrix} \mathbf{Y}_1 & \mathbf{Y}_2 & \ldots & \mathbf{Y}_\beta \\ \mathbf{Y}_2 & \mathbf{Y}_3 & \ldots & \mathbf{Y}_{\beta+1} \\ . & . & . & . \\ \mathbf{Y}_\alpha & \mathbf{Y}_{\alpha+1} & \ldots & \mathbf{Y}_{\alpha+\beta-1} \end{bmatrix} = \mathbf{P}_\alpha\mathbf{Q}_\beta \tag{8}$$

where $\mathbf{P}_\alpha = [\mathbf{C}, \mathbf{CA}, \mathbf{CA}^2, \ldots, \mathbf{CA}^{\alpha+shift-1}]^T$ is the observability matrix and $\mathbf{Q}_\beta = [\mathbf{B}, \mathbf{AB}, \mathbf{A}^2\mathbf{B}, \ldots, \mathbf{A}_\beta^{+shift-1}\mathbf{B}]$ is the controllability matrix; shift is set to 10 in this paper according to experience. The last row and column blocks are time-shifted by "*shift*" times more than normal shifting time to calculate consistency indicators. If the size of the Hankel matrix is too small, then some of the physical modes can be missed. On the contrary, if the size of the Hankel matrix is unnecessarily too large, then the system matrix $\mathbf{A}$ can be tainted with a significant number of nonphysical modes.

To realize the underlying state-space model, it is necessary to apply singular value decomposition (SVD) to the Hankel matrix as follows

$$\mathbf{H}(0) = \mathbf{R}\Sigma\mathbf{S}^T \tag{9}$$

where $\mathbf{R}$ and $\mathbf{S}$ indicate the left and right eigenvectors of $\mathbf{H}(0)$ and Σ is a diagonal matrix that has singular values along its diagonal terms. The rank of the Hankel matrix is determined by checking the number of non-zero singular values. The row and column block is replaced with the triplet for the discrete-time system, which can be identified as follows (Juang *et al.* 1985)

$$\widehat{\mathbf{A}} = \Sigma_n^{-1/2}\mathbf{R}_n^T\mathbf{H}(1)\mathbf{S}_n\Sigma_n^{-1/2}$$

$$\widehat{\mathbf{B}} = \Sigma_n^{1/2}\mathbf{S}_n^T\mathbf{E}_r$$

$$\widehat{\mathbf{C}} = \mathbf{E}_m^T\mathbf{R}_n\Sigma_n^{1/2} \tag{10}$$

where $\mathbf{R}_n$ and $\mathbf{S}_n$ are formed by eliminating columns of $\mathbf{R}$ and $\mathbf{S}$ corresponding to relatively small or negligible singular values. It is noted that the relationships $\mathbf{R}_n^T\mathbf{R}_n = \mathbf{I}$ and $\mathbf{S}_n^T\mathbf{S}_n = \mathbf{I}$ are established. $\mathbf{H}(1)$ is a time-shifted Hankel matrix from $\mathbf{H}(0)$. $\mathbf{E}_m^T = [\mathbf{I} \ \mathbf{0}]$ and $\mathbf{E}_r^T = [\mathbf{I} \ \mathbf{0}]$ are used for selecting the system matrices $\widehat{\mathbf{B}}$ and $\widehat{\mathbf{C}}$ from extended controllability and observability matrices. The eigenvalues and eigenvector matrix of $\widehat{\mathbf{A}}$ can be found by solving the eigenvalue problem, which is defined as

$$\widehat{\mathbf{A}}\Psi = \Psi\Lambda \tag{11}$$

where Ψ indicates the eigenvector matrix and $\Lambda = \mathrm{diag}(\lambda_1, \lambda_2,\ldots, \lambda_n)$ indicates the diagonal matrix containing eignevalues. Next, the eigenvalues, modal participation factor, and mode shapes can be obtained as

$$\Lambda = \Psi^{-1}\widehat{\mathbf{A}}\Psi \ ; \quad \mathbf{B}' = \Psi^{-1}\widehat{\mathbf{B}} \ ; \quad \mathbf{C}' = \widehat{\mathbf{C}}\Psi \tag{12}$$

where $\mathbf{B}'$ indicates the modal participation factors and $\mathbf{C}'$ indicates the mode shapes. The natural frequency and the modal damping ratio are obtained after transforming to s-plane; that is, $s_n = \ln(\lambda_n)/\Delta t$, where Δt is the sampling time step size. Lastly, the modal damping ratio and the damped natural frequencies in hertz are obtained as follows

$$\zeta_n = -\frac{\mathrm{Re}\{s_n\}}{\sqrt{\mathrm{Re}\{s_n\}^2 + \mathrm{Im}\{s_n\}^2}} \times 100(\%) \ ; \quad f_{dn} = \frac{\mathrm{Im}\{s_n\}}{2\pi} \tag{13}$$

where n means the nth mode; $\mathrm{Re}\{\cdot\}$ and $\mathrm{Im}\{\cdot\}$ indicates the real and imaginary parts of a complex variable; f_{dn} indicates damped natural frequency of the nth mode.

However, in practical implementations, ERA analysis can contain a significant number of computational (e.g., nonphysical) modes due to nonlinearity, noise effect, inadequate excitations, or other factors. Several consistency indicators are introduced to distinguish the nonphysical modes from identified modal characteristics through ERA analysis.

3. Damage detection method by parameter subset selection method

Model-based damage detection frequently becomes ill-posed inverse problems in which a large number of damage parameters are to be identified based on modal properties represented in a global sense. To alleviate challenges from the ill-posedness, a new parameter subset selection method is introduced; the major advantage of the new method is its ability to efficiently locate multiple damage locations. In the new method, the sensitivity matrix of the dynamic residual force vector is derived and is utilized for detecting damage.

3.1 Sensitivity matrix of dynamic residual force vector

Herein it is assumed that structural damage can be modeled as a reduction of Young's modulus in each finite element. The problem is theoretically formulated in a general way before selecting the specific structural terms to use. The residual function is expressed as

$$J = \|\mathbf{z}_m - \mathbf{z}(\theta)\|^2 \tag{14}$$

where $\mathbf{z}_m$ is the vector consisting of values obtained from measured data and $\mathbf{z}(\theta)$ consists of the same quantities as a function of damage parameters, θ. Because the residual function is a nonlinear function of the damage parameters, it is a combinatorial optimization problem in which θ is sought by minimizing this function. Dropping higher order terms of Taylor series of $\mathbf{z}_m$, a linearized $\mathbf{z}_m$ equation is given by

$$\mathbf{S}\theta = \mathbf{b} \tag{15}$$

where $\mathbf{b} = \mathbf{z}_m - \mathbf{z}(0)$ is the difference in the measured values between the measured and predicted damaged states and $\mathbf{S} = [\nabla_{\theta'} z_1(\theta')|_{\theta' = 0} \nabla_{\theta'} z_2(\theta')|_{\theta' = 0} \nabla_{\theta'} z_p(\theta')|_{\theta' = 0}]$. In (Titurus *et al.* 2003, Song *et al.* 2009), $\mathbf{z}_m$ was defined as stacked fundamental modal quantities such as eigenvalues and eigenvectors. However, in this paper, $\mathbf{z}_m$ is defined as a residual force vector. For instance, the ith residual force vector for an undamaged structure is given by

$$\mathbf{R}_i = \mathbf{K}\varphi_i - \lambda_i \mathbf{M}\varphi_i \tag{16}$$

where $\mathbf{K}$ and $\mathbf{M}$ are the stiffness and mass matrices of the structure, respectively. In practical applications of the proposed method, the effect of the measurement error on its performance is more pronounced than the modeling errors.

Taking the derivative of the residual force vector with respect to the jth damage parameter, sensitivities of the residual force vector can be expressed as

$$\frac{\partial \mathbf{R}_i}{\partial \theta_j} = \frac{\partial \mathbf{K}}{\partial \theta_j}\varphi_i + \mathbf{K}\frac{\partial \varphi_i}{\partial \theta_j} - \frac{\partial \lambda_i}{\partial \theta_j}\mathbf{M}\varphi_i - \lambda_i \mathbf{M}\frac{\partial \varphi_i}{\partial \theta_j} \tag{17}$$

It should also be noted that the mass matrix is assumed to not change. Thus, the sensitivity of the eigenvalues and mode shapes are calculated as in (Fox *et al.* 1968). However, because the mass matrix is constant, the second term in the sensitivity of the mode shapes will vanish. Therefore, the sensitivity matrix $\mathbf{S}$ in terms of the residual force vectors is

$$\mathbf{S} = \begin{bmatrix} \dfrac{\partial \mathbf{R}_1}{\partial \theta_1} & \dfrac{\partial \mathbf{R}_1}{\partial \theta_2} & . & \dfrac{\partial \mathbf{R}_1}{\partial \theta_p} \\[2ex] \dfrac{\partial \mathbf{R}_2}{\partial \theta_1} & \dfrac{\partial \mathbf{R}_2}{\partial \theta_2} & . & \dfrac{\partial \mathbf{R}_2}{\partial \theta_p} \\[2ex] . & . & . & . \\[1ex] \dfrac{\partial \mathbf{R}_m}{\partial \theta_1} & \dfrac{\partial \mathbf{R}_m}{\partial \theta_2} & . & \dfrac{\partial \mathbf{R}_m}{\partial \theta_p} \end{bmatrix} \in \mathbf{R}^{(neq \times m) \times (p)} \tag{18}$$

where *neq*, *m* and *p* are, respectively, the number of degrees of freedom, the number of measured modes, and the number of damage parameters. The $\mathbf{b}$ vector is also calculated by

$$\mathbf{b}_i = \mathbf{R}_{di} - \mathbf{R}_{ui}$$

$$\text{where} \quad \mathbf{R}_{di} = \mathbf{K}\varphi_{di} - \lambda_{di}\mathbf{M}\varphi_{di} \tag{19}$$

where λ_{di} and φ_{di} are the measured eigenvalues and mode shapes of the damaged structure, respectively. Because the residual force vector for an undamaged structure, $\mathbf{R}_{ui}$ will be approximately equal to the zero vector, residual values of the $\mathbf{b}$ vector originate from $\mathbf{R}_{di}$. The next problem is finding the subset of parameters that will minimize the residuals within these equations. Because the number of rows of the $\mathbf{S}$ matrix is greater than the number of columns, the problem is ill-posed in an overdetermined sense. To correct for this, the parameter subset selection method is employed for purposes of regularization, as described in the following section.

3.2 Regularization through parameter subset selection method

In the identification of damage parameters, sub-optimal problems are often sequentially formulated using the forward selection approach (Lallement *et al.* 1990). In each sub-optimal problem, one damage parameter is selected out of the remaining damage parameters. The difference of measured data, $\mathbf{b}$, in Eq. (19) can be viewed as a linear combination of a set of column vectors within the $\mathbf{S} = [\mathbf{a_1} \ \mathbf{a_2} \ ... \ \mathbf{a}_p]$ matrix using

$$\mathbf{b} = \sum_{j=1}^{p} \theta_j \mathbf{a}_j \tag{20}$$

where p indicates the number of damage parameters and a_j is the jth column of the $\mathbf{S}$ matrix. Overall, the main task of forward selection is to select a column vector in the $\mathbf{S}$ matrix that best represents the residual vector $\mathbf{b}$, that is, yields the minimum value of the resulting residual function

$$J_j = \left\| \mathbf{b} - \mathbf{a}_j^e \theta_j \right\|^2 \tag{21}$$

where the summation rule with respect to j is not applied here and the least square estimate $^e\theta_j$ of the jth parameter can be obtained by taking a derivative of $J = \left\| \mathbf{b} - \mathbf{a}_j^e \theta_j \right\|^2$ with respect to θ_j as

$$^e\theta_j = \frac{\mathbf{a}_j^T \mathbf{b}}{\mathbf{a}_j^T \mathbf{a}_j} \tag{22}$$

Finding the minimum value of the residual function $J = \left\| \mathbf{b} - \mathbf{a}_j^e \theta_j \right\|^2$ is equivalent to finding a vector $\mathbf{a}_j$ that forms the minimum angle with the vector $\mathbf{b}$. This procedure seeks the best basis vector $\mathbf{a}_j$ that is closest to the damage residual vector $\mathbf{b}$. If the first basis vector $\mathbf{a}_{j1}$ and its corresponding damage parameter θ_{j1} are found, Gram-Schmidt orthogonalization is generally performed on the remaining column vectors to ensure a well-conditioned sub-matrix of $\mathbf{S}$. A vector orthogonal to the first vector is produced by taking the original second vector and projecting out the component of the vector that lies along the first vector. This task is accomplished through the following equations

$$\mathbf{a}_j \leftarrow \mathbf{a}_j - \alpha_j \alpha_{ji} \quad \text{and} \quad \mathbf{b} \leftarrow \mathbf{b} - \mathbf{a}_{j1}{}^e\theta_{j1}$$

$$\text{where} \quad \alpha_j = \mathbf{a}_{j1}^T \mathbf{a}_j / \mathbf{a}_{j1}^T \mathbf{a}_{j1} \tag{23}$$

where α_j is the component of the vector $\mathbf{a}_j$ that lies along the first vector and $^e\theta_j$ can be calculated by Eq. (22). After orthogonalization, the residual function in Eq. (21) for each parameter j is

calculated and the minimum value is chosen as follows

$$\min(\{J_2, J_3, \ldots, J_p\}) \rightarrow \mathbf{a}_{j2} \quad \text{and} \quad \theta_{j2} \tag{24}$$

Equivalently, the minimum angle between orthogonalized column vector $\mathbf{a}_j$ and residual vector $\mathbf{b}$ can be sought. Therefore, the angle can be described as

$$\phi = \cos^{-1}\left(\sqrt{\frac{(\mathbf{a}_j^T \mathbf{b})^2}{(\mathbf{a}_j^T \mathbf{a}_j)(\mathbf{b}^T \mathbf{b})}}\right) \tag{25}$$

This iterative procedure is continued in order to identify m damage parameters while retaining the parameters chosen in the previous steps. When a total of m damage parameters are selected in the subset, the residual sum of squares is defined as

$$RSS_m = \left\| b - \sum_{i=1}^{m} \mathbf{a}_{j_i} {}^e\theta_{j_i} \right\|^2 \tag{26}$$

where ${}^e\theta_j$ is the least squares estimator for the jth parameter, as found in Eq. (22). Efroymson suggested a stepwise regression algorithm that provides a basis by which to decide whether a new parameter should be included in the subset (Efroymson 1960). If $[\theta_1, \theta_2, \ldots, \theta_m]$ are already selected as damage parameters and a new parameter θ_{m+1} is chosen for evaluation, then the F-to-enter statistic can be expressed as

$$F_a = \frac{RSS_m - RSS_{m+1}}{RSS_{m+1}/(n-m-1)} \tag{27}$$

where RSS indicates the residual sum of squares and n is the number of total parameters. If the F_a value is greater than a predetermined value (F_{in}), the parameter is included in the subset. If the criterion is not met, the parameter is excluded.

4. Damage quantification by steady state genetic algorithm

Once damage detection has been achieved by the subset selection method, the extent of damage can be evaluated; this evaluation of damage extent plays an important role in the subsequent decision-making process. When dealing with large-scale finite element models in genetic algorithms, the evaluation of cost functions requires an enormous computational time. In this study, the steady state genetic algorithm (SSGA) was used to overcome the demand for considerable amounts of computational time.

4.1 Modal flexibility matrix for cost function

A finite element model containing damage parameters is used for the identification model. The damage parameters in the model are related to changes in the stiffness matrix and/or mass matrix. It is assumed that structural damage is described as a reduction in Young's modulus (E) for each finite element. Thus, the global stiffness matrix can be expressed as the summation of damaged and undamaged element stiffness matrices, where the local element stiffness is multiplied by a reduction factor as

$$[\mathbf{K}] = \sum_{i=1}^{nelem} (1 - \theta_i)[\mathbf{k}]_i \tag{28}$$

where 'nelem' is the total number of elements in the analytical model; θ_i is the damage parameter associated with the ith element, which equals zero for the healthy state and unity for the complete damage state; and [$\mathbf{K}$] is the structural stiffness matrix, where [$\mathbf{K}$] is assembled from the elemental stiffness matrices [$\mathbf{k}$]$_i$ as expressed in Eq. (28). The modal flexibility matrix is employed as a cost function. With its particular sensitivity to structural damage, the modal flexibility methodology is numerically advantageous to use over the flexibility matrix because it does not require the inverse of the modal matrix. Therefore, the computation time is significantly less demanding. The modal flexibility matrix can be derived as

$$\mathbf{F} = \mathbf{\Phi}\mathbf{\Lambda}^{-1}\mathbf{\Phi}^T \tag{29}$$

where $\mathbf{\Phi}$ is the mode shape matrix and $\mathbf{\Lambda}$ represents the diagonal matrix containing the square of the modal frequencies. Underlying assumption in Eq. (29) is that the mode shape matrix should be mass-normalized. In practical applications, estimating masses of actual structures could be erroneous resulting in negative effects on the damage quantification. Therefore, precise determination of masses of the monitored structure is required in order to use the modal flexibility matrix as an objective function. The difference between the tested model and the analytical model can then be utilized as an objective function for damage quantification

$$\Pi(\theta) = \left\| \mathbf{F}_{exp} - \mathbf{F}_{updated}(\theta) \right\|_{Fro} \tag{30}$$

where θ is the vector depicting the damage parameters, $\| \;\|_{Fro}$ represents the Frobenius norm for the residual matrix, $\mathbf{F}_{exp}$ indicates modal flexibility matrix from the identified results, and $\mathbf{F}_{updated}$ is the modal flexibility matrix calculated from the analytical model with vector damage parameters.

4.2 Steady State Genetic Algorithm (SSGA)

In conventional GAs, such as the simple genetic algorithm (SGA), the entire population is replaced in each generation through the GA operators. Therefore, the reproduction process for the SGA will require an enormous amount of computational time because it has to evaluate the cost function for the entire population. However, the steady state genetic algorithm (SSGA) based on non-generational evolution paradigm can achieve equivalent performance as the SGA with elitism and scaling of fitness values, and it saves a tremendous amount of computational time because it evaluates only a small percentage of the entire population during each generation. By considering this advantage of SSGA with the idea of modeling to generate alternatives (MGA), Caicedo *et al.* (2008) were able to develop a combined SSGA-MGA algorithm (Caicedo and Yun 2011).

Unlike the SGA, the SSGA significantly simplifies reproduction process for new offspring. After initialization of the parent population, all chromosomes are ranked according to their fitness values. Thus, the cost function must be computed for the entire population at the beginning, which is a one-time computation. However, after the parent population is evaluated, the two chromosomes with the highest fitness values are chosen for crossover and therefore produce new offspring. The new

offspring replace the two chromosomes with the worst fitness values. After that, to ensure diversity, mutation is applied to the new offspring. Finally, cost functions of only two new mutated offspring are evaluated in the SSGA algorithm. Computation of the cost function of a chromosome requires recalculations of elemental stiffness matrices, eigenvalues, mode shapes and modal flexibility matrix with a new set of element-by-element damage parameters. Considering that other genetic algorithms require computations of cost function of every chromosome in each generation, this characteristic of the SSGA is very beneficial, as it can significantly reduce the computational effort. Moreover, the population evolves steadily toward optimal solutions without endangering the highest fit schemata that already exists in the population.

5. Illustrative numerical examples and discussions

In this example, the proposed method from modal identification to damage detection has been verified with numerical examples, which consider environmental effects such as damping level and sensor noise and error.

5.1 Example truss structure and numerical modeling

In this example, a 14-bay planar truss is selected to demonstrate the performance of the proposed SHM methodology for the purpose of damage diagnosis. The truss is modeled using 53 truss elements with 28 nodes, as shown in Fig. 2. The total length of the structure is 5.56 m (each of the 14 bays is 0.40 m in length) and the height of the truss structure is 0.40 m. The members are steel bars with a tube cross section having an inner diameter of 3.1 mm and an outer diameter of 17.0 mm. The physical properties are as follows: the elastic modulus of the material is equal to 1.999×10^{11} N/m^2; and the mass density is equal to 7,827 kg/m^3. The members are connected using pinned joints. There are two supports at each end of the structure: a pin support at the left end and a pinned roller support at the right end. The resulting numerical model has 53 DOFs. In this paper, sensors are assumed to be placed at each node.

The truss structure has been modeled as a linear time-invariant model in state-space form. A classical damping matrix of the structure is formed using a modal damping ratio applied to all the modes. For numerical simulations under ambient excitation, a built-in MATLAB function (*lsim.m*) is used.
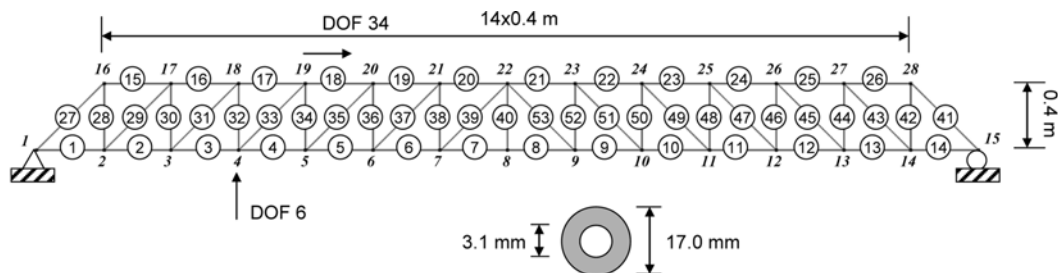

Fig. 2 2D finite element model (the circled number indicates element number) of a fourteen-bay planar truss

Table 1 Tested damage scenarios

Damage Scenarios	Damaged Elements	Damage Severity	Distribution	# of Damaged Element
1	32	90% loss of section	-	Single
2	7, 8, 40	90% loss of section	Grouped	Multiple
3	13, 20, 33	90% loss of section	Distributed	Multiple
4	8, 18	10% loss of section	Distributed	Multiple
5	8, 18	15% loss of section	Distributed	Multiple

5.2 Damage scenarios

Five damage scenarios are assumed herein. The first damage scenario assumes single severe damage at the element number 32, representing 90% loss of the cross section. The second damage scenario is intended to be a multiple severe damage (90% loss of cross section) case where the damaged elements (element numbers 7, 8, and 40) are located nearby. The third damage scenario assumes a severe multiple damage (90% loss of cross section) case in which the damaged elements (element numbers 13, 20, and 33) are evenly distributed along the span. The fourth damage scenario assumes a challenging case in which two elements are lightly damaged (10% loss of cross section; element numbers 8 and 18). The fifth scenario is also challenging case in which noisy ambient data will be used for identifying lightly damaged elements (15% loss of cross section; element numbers 8 and 18). The current damage scenarios are summarized in Table 1.

5.3 Damage diagnosis under ambient vibration data

Modal Identification: In this example, modal properties (e.g., natural frequency, mode shapes, damping ratios and modal participation factors) are identified using the NExT/ERA method under ambient vibration. The modal identification assumes a constant modal damping ratio of 0.1% for every mode. Natural frequencies of the numerical model are within a range of 31.93 Hz to 2979.77 Hz. By using the sampling frequency 2028 Hz, the ambient vibration measurements are purposely set to have the highest identifiable natural frequency that is less than 1024 Hz by which total 19 modes are identifiable. A Gaussian white noise excitation is applied in a vertical direction at node 4, which is corresponding to DOF 6. A typical acceleration measurement from the input excitation is shown in Fig. 3(a). For comparison, the impulse response function is obtained as in Fig. 3(b) by inverse fast Fourier transform (IFFT) of the frequency response function (FRF). Fig. 4(a) shows a CPSD function between the response at a reference DOF 6 and the response at DOF 34. For the calculation of the CPSD, 4,096 points are used for each window and a total of 360 windows are averaged.

Accuracy of the modal identification is assessed using the consistency mode indicator (Pappa *et al.* 1993). According to the test, the ERA analyses showed better performances with lightly damped structures than with highly damped structures. For the current analysis, the size of the Hankel matrix is fixed to have 1060 × 530.

Damage Detection and Quantification: Using the identified first 10 modal properties, multiple locations of damage are identified by the proposed parameter subset selection method prior to quantification of the damage severity. In the parameter subset selection method, threshold values for
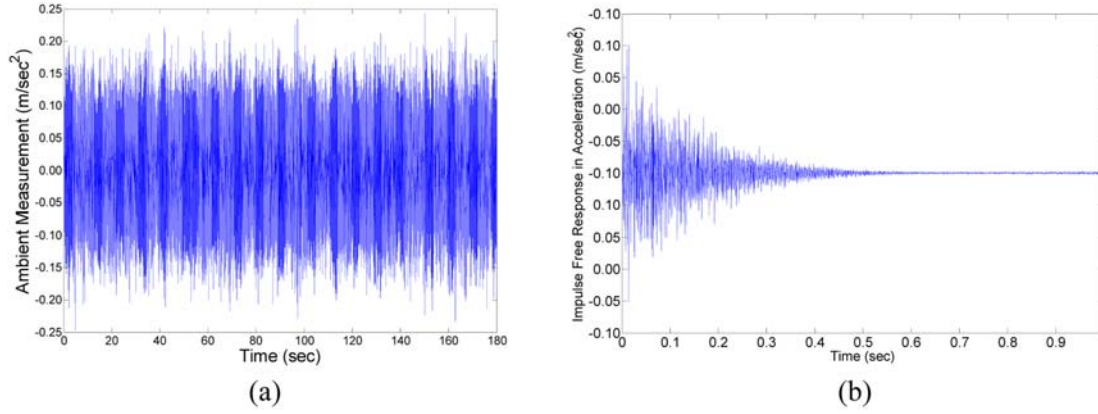
Fig. 3 (a) A typical ambient vibration measurements in acceleration and (b) a typical original impulse free response from IFFT of FRFs
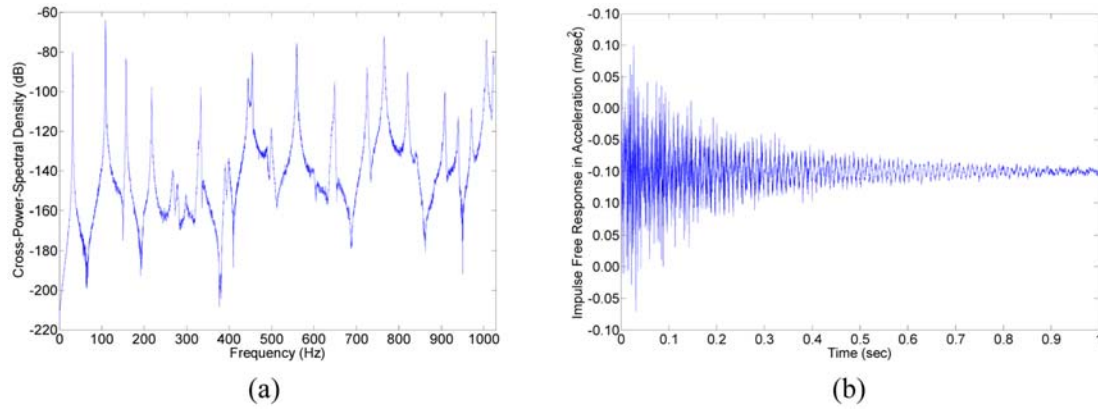

Fig. 4 (a) A typical cross-power-spectral density function between the response of a reference DOF 6 and the response of DOF 34 and (b) its corresponding reconstructed impulse free response through NExT technique

the F-to-enter statistic (which is calculated in Eq. (27)) are determined by plotting the F-to-enter ratios during iterative steps of subset selection as shown in Fig. 5, since they are dependent on the given problems. Damaged elements are selected for each damage scenario in Fig. 5. If an undamaged element is selected, the F-to-enter statistic abruptly decreases. In the case of damage scenario 1, the F-to-enter ratio plot apparently indicates the presence of a single damaged element as shown in Fig. 5(a). However, for the sake of safe selection, two elements are selected as the suspicious damaged elements. In the case of damage scenario 2, a total of five elements are chosen based on the threshold value of 0.35. The parameter subset selection method is shown to be capable of selecting all of the assumed damage locations.

Since a minimum angle between the orthogonalized column vector of the sensitive matrix and residual vector in Eq. (25) is sought during iterations of the parameter subset selection, elements having smaller subspace angles with residual vector are selected as potentially damaged elements.
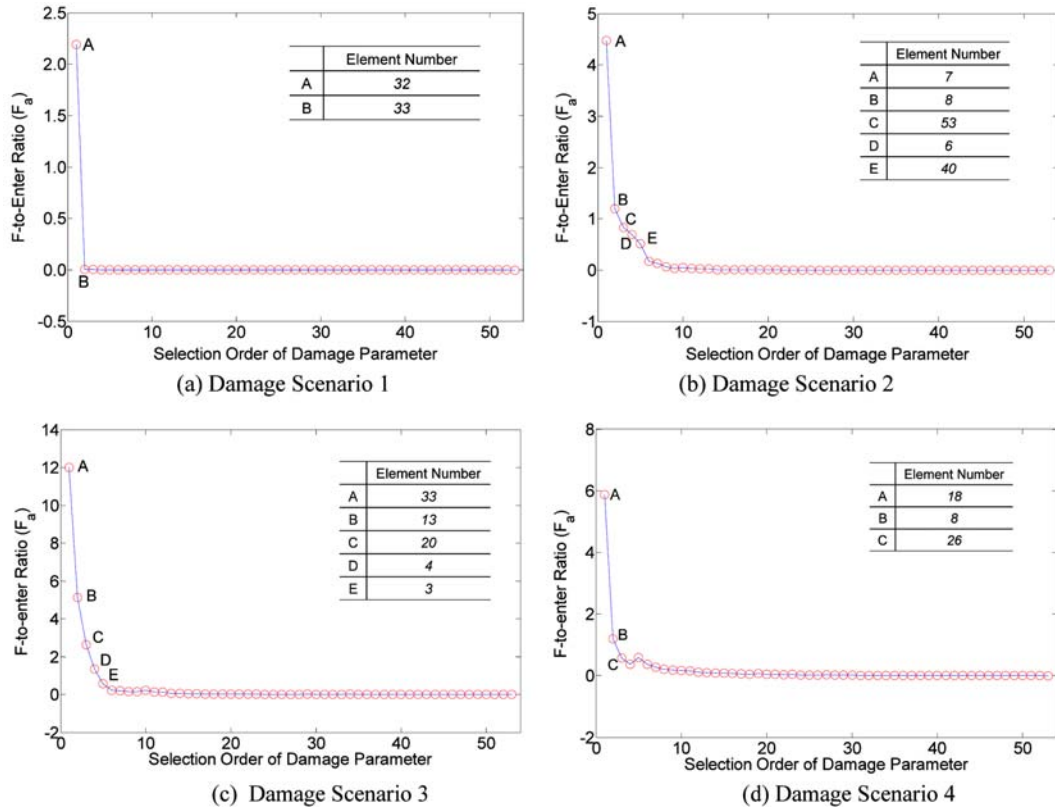
Fig. 5 F-to-enter ratios showing damaged elements and their order of selection by parameter subset selection method

Figs. 6(a), 6(c), 6(e) and 6(g) show "90°-subspace angle" for all the elements after the selection process. In terms of the subspace angle, damaged elements were distinguishable from other undamaged elements. Apparently, it is advantageous that the parameter subset selection method could efficiently reduce the number of damage parameters before solving the optimization problem for damage quantifications. Figs. 6(b), 6(d), 6(f) and 6(h) show the extent of the damage determined by the steady state genetic algorithm for the damage scenarios 1 through 4. It is notable that although undamaged elements are erroneously selected, the steady state genetic algorithm is capable of both regulating incorrectly chosen elements and measuring extents of the damage. For example, elements 6 and 53 were selected as potentially damaged elements by the parameter subset selection method in the case of damage scenario 2. However, while searching the extent of damage through the genetic algorithm, they were identified as undamaged elements or elements with minor changes in structural stiffness. Damage scenario 4 is a lightly damaged case in which a 10% loss of cross sections of two elements is assumed. As shown in Fig. 6, their damage locations and the severity of the damage were reasonably identified. The proposed damage diagnosis methodology was shown to be an excellent tool when combined with the modal identification for structural health monitoring through the testing under single, multiple, spatially grouped, distributed, severely and lightly damaged cases.

(a) Damage Location for Damage Scenario 1

(b) Severity of Damage for Damage Scenario 1

(c) Damage Location for Damage Scenario 2

(d) Severity of Damage for Damage Scenario 2

(e) Damage Location for Damage Scenario 3

(f) Severity of Damage for Damage Scenario 3

(g) Damage Location for Damage Scenario 4

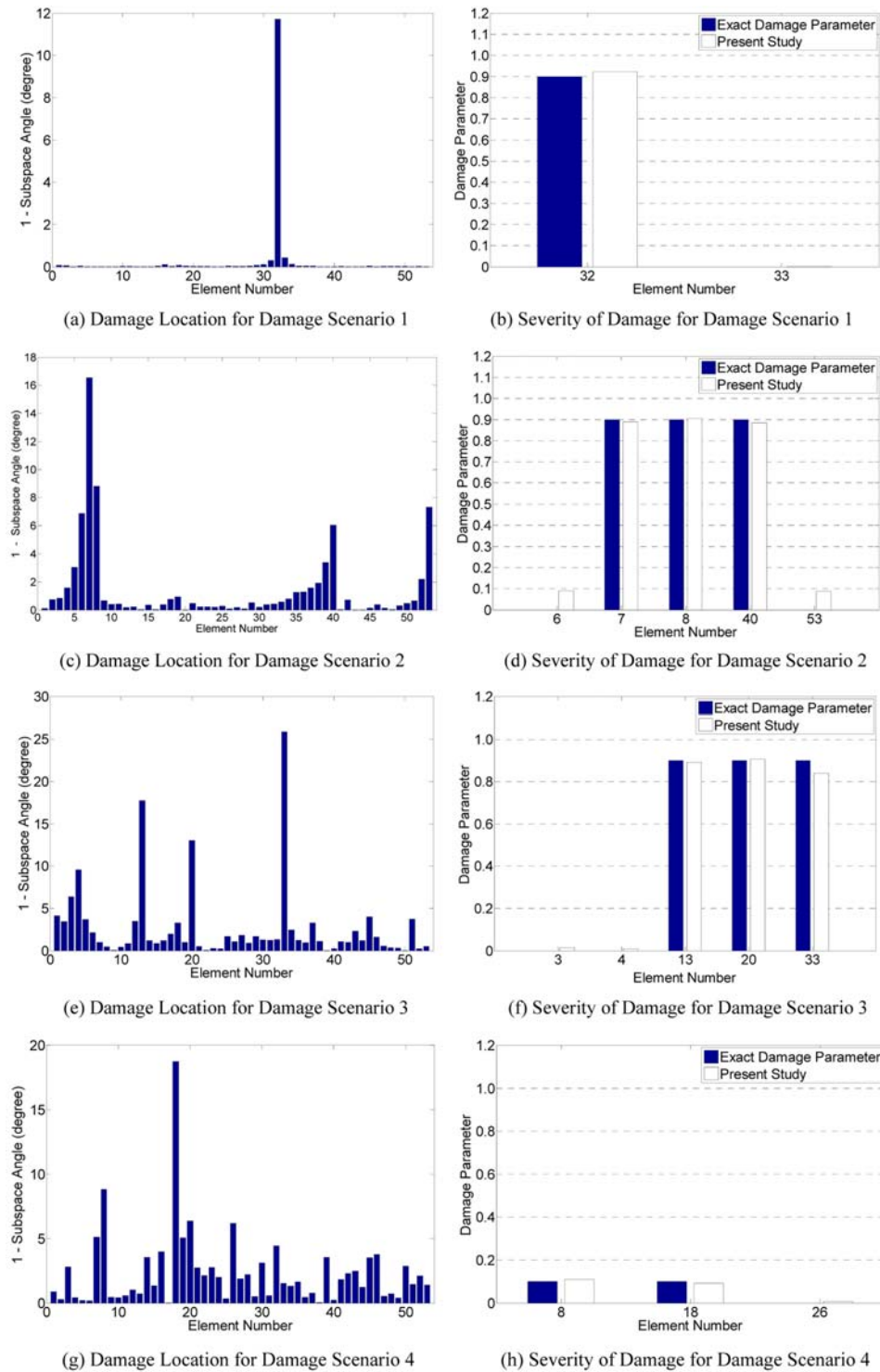(h) Severity of Damage for Damage Scenario 4

Fig. 6 Damage locations identified by parameter subset selection method and damage extent determined by steady state genetic algorithm for damage scenario 1, 2, 3 and 4; First 10 mode shapes were used

5.4 Damage diagnosis under noisy ambient vibration

In this section, the suggested damage diagnosis method has been demonstrated under noisy ambient measurement data. The modal identification assumes a constant modal damping ratio of 0.1% for every mode in order to study the effect of the sensor noise alone on the accuracy of the identification results. Before beginning the modal identification, acceleration response data are contaminated with zero-mean Gaussian broadband noise signals. Three noise levels – in which the signal-to-noise ratio (SNR) is equal to 20 dB, 10 dB, and 1 dB – and a noise-free case are considered. The SNR is defined as

$$SNR = 10\log_{10}\left(\frac{\sigma_S^2}{\sigma_N^2}\right) \tag{31}$$

Table 2 Modal identification results for different damage scenario and effects of sensor noise (1st mode)

Damage Scenario	Accuracy	Noise-Free Data	SNR = 20 dB	SNR = 10 dB	SNR = 1 dB
1	$100 \times |f_{true} - f_{id}|/f_{true}$	0.1376	0.1449	0.2292	0.0219
	$MAC(\varphi_{true}, \varphi_{id})$	0.9999	0.9999	0.9998	0.9979
2	$100 \times |f_{true} - f_{id}|/f_{true}$	0.0194	0.0184	0.0715	0.0475
	$MAC(\varphi_{true}, \varphi_{id})$	0.9999	0.9999	0.9998	0.9921
3	$100 \times |f_{true} - f_{id}|/f_{true}$	0.1645	0.1938	0.1508	0.1456
	$MAC(\varphi_{true}, \varphi_{id})$	0.9999	0.9999	0.9999	0.9996
4	$100 \times |f_{true} - f_{id}|/f_{true}$	0.0929	0.0717	0.0749	0.1136
	$MAC(\varphi_{true}, \varphi_{id})$	0.9999	0.9999	0.9999	0.9947
5	$100 \times |f_{true} - f_{id}|/f_{true}$	0.1388	0.1496	0.1365	0.1668
	$MAC(\varphi_{true}, \varphi_{id})$	0.9999	0.9999	0.9999	0.9989

Table 3 Modal identification results for different damage scenario and effects of sensor noise (10th mode)

Damage Scenario	Accuracy	Noise-Free Data	SNR = 20 dB	SNR = 10 dB	SNR = 1 dB
1	$100 \times |f_{true} - f_{id}|/f_{true}$	0.0083	0.0037	0.0266	0.1538
	$MAC(\varphi_{true}, \varphi_{id})$	0.9980	0.9994	0.9896	0.7470
2	$100 \times |f_{true} - f_{id}|/f_{true}$	0.0002	0.0069	0.0016	0.0039
	$MAC(\varphi_{true}, \varphi_{id})$	0.9999	0.9999	0.9996	0.9995
3	$100 \times |f_{true} - f_{id}|/f_{true}$	0.0034	0.0081	0.0060	0.0099
	$MAC(\varphi_{true}, \varphi_{id})$	0.9999	0.9999	0.9971	0.9999
4	$100 \times |f_{true} - f_{id}|/f_{true}$	0.0107	0.0077	0.0030	0.0047
	$MAC(\varphi_{true}, \varphi_{id})$	0.9989	0.9991	0.9993	0.9905
5	$100 \times |f_{true} - f_{id}|/f_{true}$	0.0059	0.0047	0.0038	0.0034
	$MAC(\varphi_{true}, \varphi_{id})$	0.9997	0.9929	0.9995	0.9986

where σ_S^2 indicates the variance of the ambient response signal and σ_N^2 indicates the variance of the zero-mean Gaussian noise added to the acceleration response. In this example, the Hankel matrix size is set to be 1060×530 (row $\times$ column) with 212 poles assumed.

Table 2 and Table 3 summarize the identification results with various levels of sensor noise for 1st and 10th modes for each damage scenario. According to the results, the results of 1st and 10th modes obtained from NExT/ERA are found to be insensitive to the sensor noise given.

For the damage scenario 2, effects of the sensor noise on the identified results are demonstrated in Fig. 7. Sensor noise is set to increase from 0.1 to 20 dB by 0.5 dB increments. Thus a total of 82 NExT/ERA analyses have been conducted. MAC values less than 0.5 are not indicated. Fig. 7 shows the effect of the sensor noise on the degree of deviations of the identified modal properties from true values up to 19th mode. According to the results, the first 10 modes are determined to be used for subsequent damage diagnosis by the proposed method.

In case of a 0.1% damping ratio, three identified modes (1, 4 and 10th modes) by NExT/ERA are plotted in a complex plane. As shown in Fig. 8, the complex modes are in phase or 180° out of phase because classical (proportional) damping is assumed. When sensor noise is considered, the collinearity of the complex modes appears to be violated. Both the sensor noise and identification accuracy of the NExT/ERA affects the collinearity of the complex modes.

To investigate effects of the sensor noise added prior to the modal identification on performances of the proposed damage diagnosis method, two cases – where sensor noise intensities have SNR that were equal to 1 dB and 0.1 dB – are considered herein. The NExT/ERA techniques identified

(a) Frequency Difference   (b) Modal Assurance Criteria MAC(φ_{true}, φ_{id})
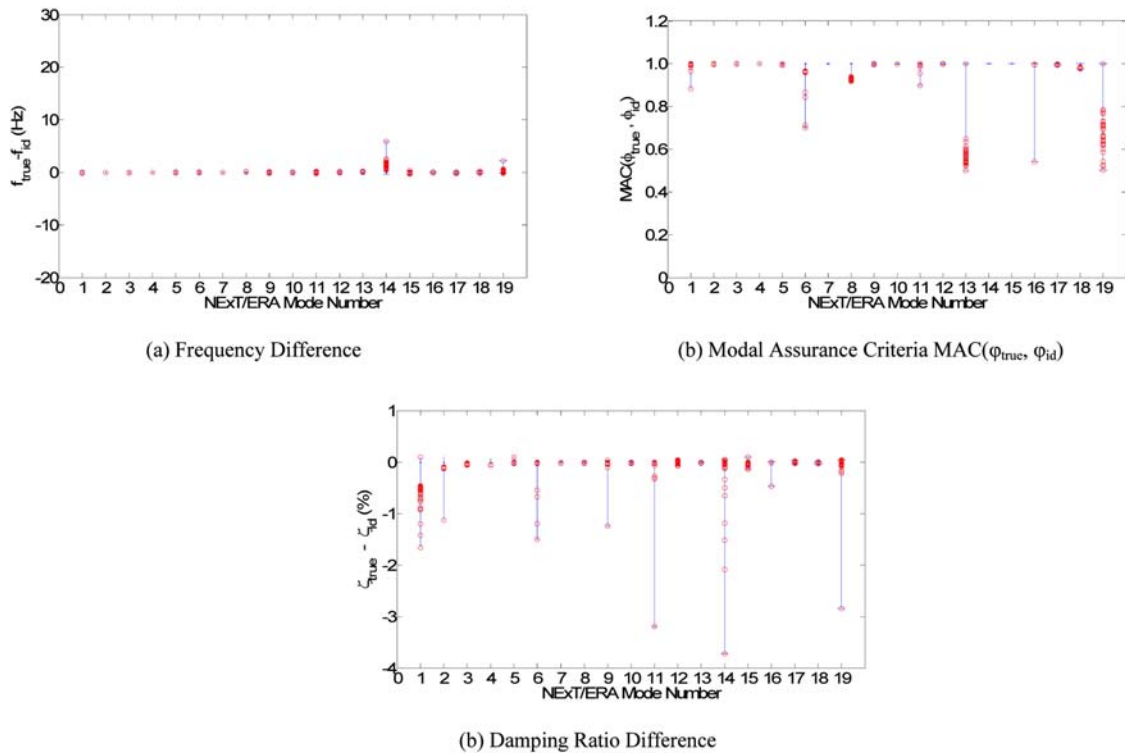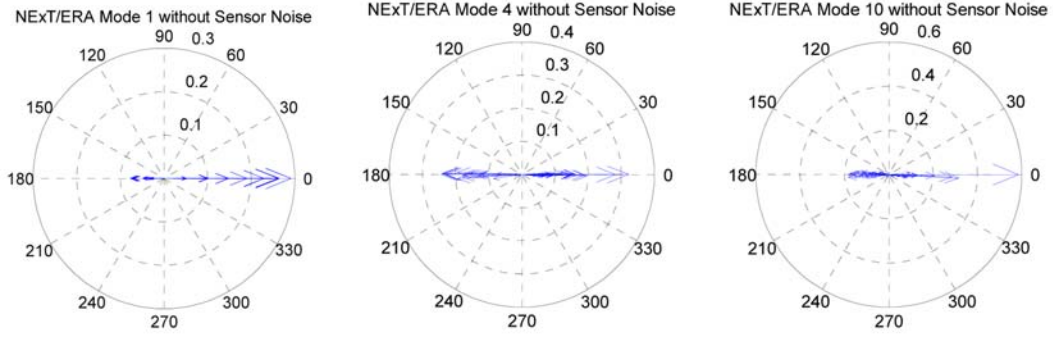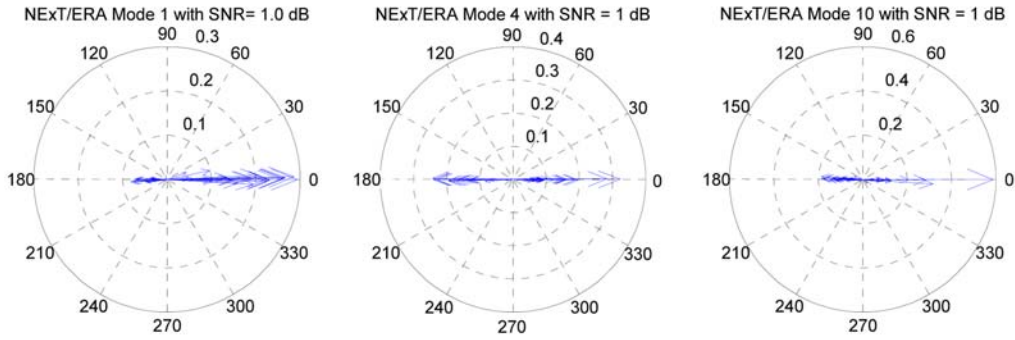
(b) Damping Ratio Difference

Fig. 7 Effects of sensor noise (SNR = 0.1 dB~20 dB with 0.5 dB increments) on NExT/ERA frequency, mode shapes and damping factor: damage scenario 2 is assumed

(a) Complex Modes without Sensor Noise

(b) Complex Modes with Sensor Noise (SNR = 1 dB)

Fig. 8 Complex modes (Mode 1, 4 and 10) identified by NExT/ERA analysis and effects of sensor noise (damage scenario 2)

Table 4 Identified results by NExT/ERA techniques with sensor noises (NExT = 360 windows averaged = 8 sec data)

Mode Number	SNR = 1dB		SNR = 0.1 dB	
	MAC(φ_{true}, φ_{id})	$100 \times |f_{true} - f_{id}|/f_{true}$	MAC(φ_{true}, φ_{id})	$100 \times |f_{true} - f_{id}|/f_{true}$
1	0.998842	0.346508	0.997222	0.369339
2	0.999946	0.017389	0.996620	0.018071
3	0.999729	0.050285	0.999116	0.021489
4	0.999945	0.013593	0.999777	0.017763
5	0.999637	0.010850	0.994431	0.001465
6	0.999046	0.006852	0.962472	0.013652
7	0.999944	0.004262	0.999426	0.013944
8	0.989088	0.002218	0.942207	0.005337
9	0.927253	0.003344	0.999612	0.000495
10	0.999820	0.012070	0.999256	0.033083

(a) Damage localization with SNR=1 dB

(b) Damage quantification with SNR=1 dB

(c) Damage localization with SNR=0.1dB

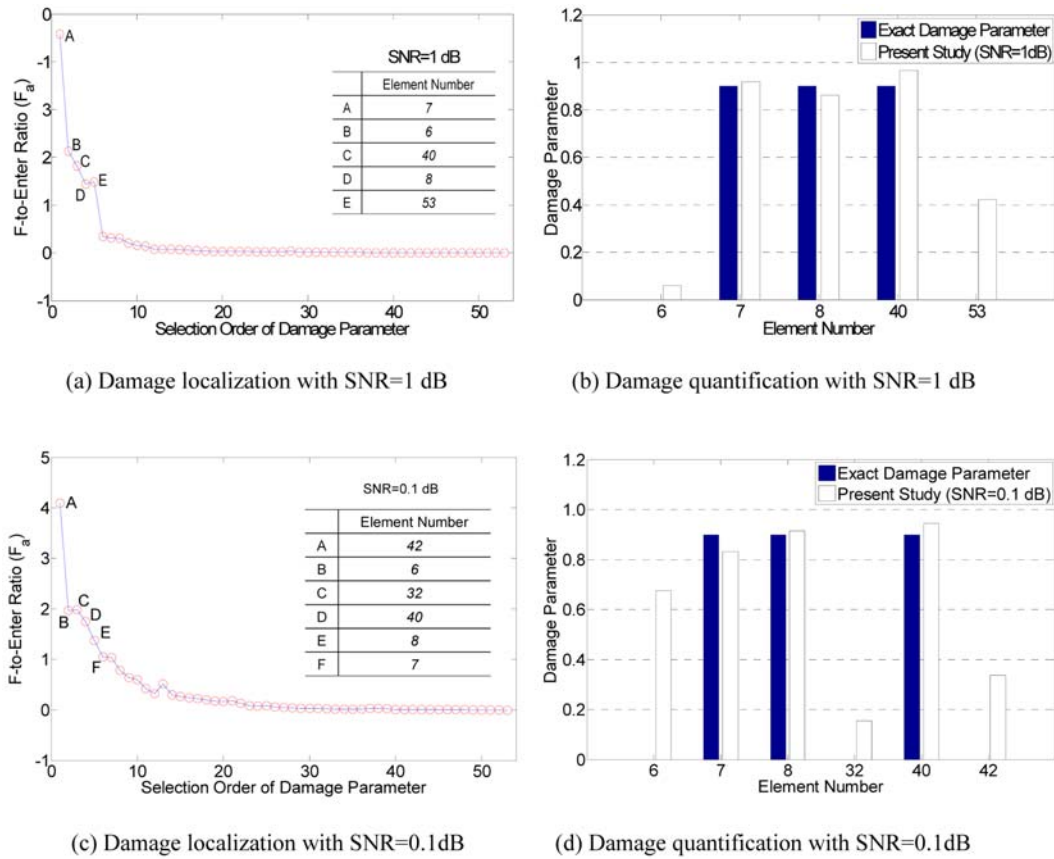(d) Damage quantification with SNR=0.1dB

Fig. 9 Selection of damaged elements and quantification of damage extent; sensor noise (SNR = 1 dB and SNR = 0.1 dB) for damage scenario 2; NExT = 360 windows averaged = 8 sec data; First 10 mode shapes were used

modal properties as shown in Table 4. The first ten modes were identified with reasonable accuracy. It is notable that the sensor noise effect on modal properties is very low, as shown in Table 4. Therefore, the proposed method will be able to identify damage locations and the damage extent with sufficient accuracy.

However, in *in-situ* modal testing, it could be difficult to obtain high quality mode shapes more than 6 modes. Therefore, the first 5 mode shapes were used for damage scenario 5. In the case of SNR = 1 dB, the parameter subset selection method chose a total of five elements (7, 6, 40, 8, and 53) as potentially damaged elements based on F-to-enter ratio plotted as in Fig. 9(a). However, in the case of SNR = 0.1 dB, a total of six elements (42, 6, 32, 40, 8, and 7) are selected. Apparently, the sensor noise causes negative effects in selecting the correct damaged elements because the identified mode shapes and natural frequencies are used in calculations of the residual vector. Since the sensor noise can also distort the modal flexibility matrix, the searching process by the steady state genetic algorithm is shown to be slightly affected by the sensor noise as shown in Figs. 9(b) and (d). However, the proposed damage diagnosis method was shown to reasonably identify damage using the identified modal properties. Moreover, considering that the assumed sensor noise

is far more intense than the normal intensity of sensor noise in practical applications (SNR = 1.0 dB ~7.0 dB), the proposed methodology is considered to be a very promising component used in structural health monitoring systems in conjunction with advanced sensor technologies such as wireless smart sensors.

For a challenging case, damage scenario 5 has been tested as shown in Fig. 10. Noise level in this case is assumed to be SNR = 20 dB. Through the parameter subset selection, 4 elements (8, 27, 18 and 33) were selected as potentially damaged ones. Actual damaged elements were successfully included in the subset. Through the damage quantification process, actual damage levels of element 8 and 18 could be reasonable estimated as shown in Fig. 10. Element 33 was successfully found to be under no damage. However, element 27 was erroneously included in the pool of damaged elements due to noise effects. Overall, the proposed method could identify all damage locations as well as their severity successfully.

As noted previously, the CPSDs from NExT technique were computed using 4096 points for FFT,
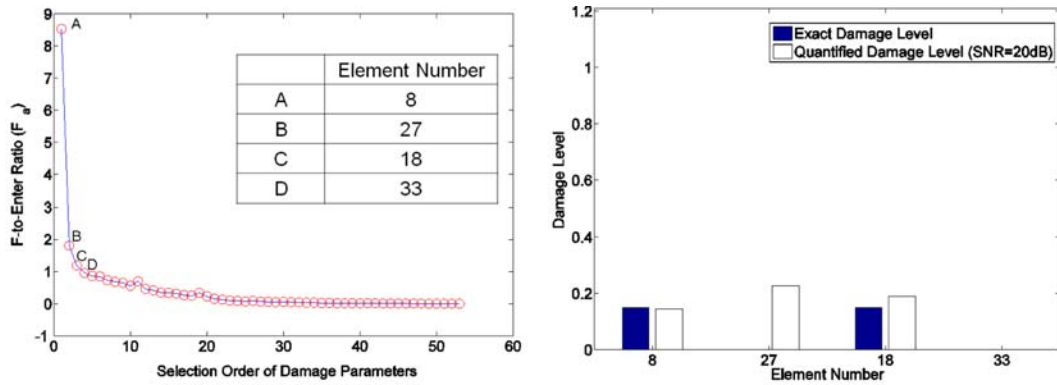

Fig. 10 Selection of damaged elements and quantification of damage extent: sensor noise (SNR = 20.0 dB) for damage scenario 5; NExT = 360 windows averaged = 8 sec data; First 5 mode shapes are used

Table 5 Identified results by NExT/ERA techniques with sensor noises (NExT = 45 windows Averaged = 8 sec data)

Mode Number	SNR = 1 dB		SNR = 0.1 dB	
	MAC(φ_{true}, φ_{id})	$100 \times |f_{true} - f_{id}|/f_{true}$	MA(φ_{true}, φ_{id})	$100 \times |f_{true} - f_{id}|/f_{true}$
1	0.973990	0.099433	0.997002	0.241695
2	0.999943	0.003364	0.999870	0.003388
3	0.999934	0.004600	0.999935	0.000367
4	0.999951	0.017042	0.999912	0.008875
5	0.999668	0.016288	0.999319	0.026852
6	0.998988	0.003036	0.999133	0.001151
7	0.999960	0.005437	0.999919	0.002621
8	0.976089	0.017154	0.986495	0.012393
9	0.999965	0.002033	0.999967	0.007010
10	0.999955	0.000354	0.999879	0.000368

(a) Damage localization with SNR=1 dB (b) Damage quantification with SNR=1 dB
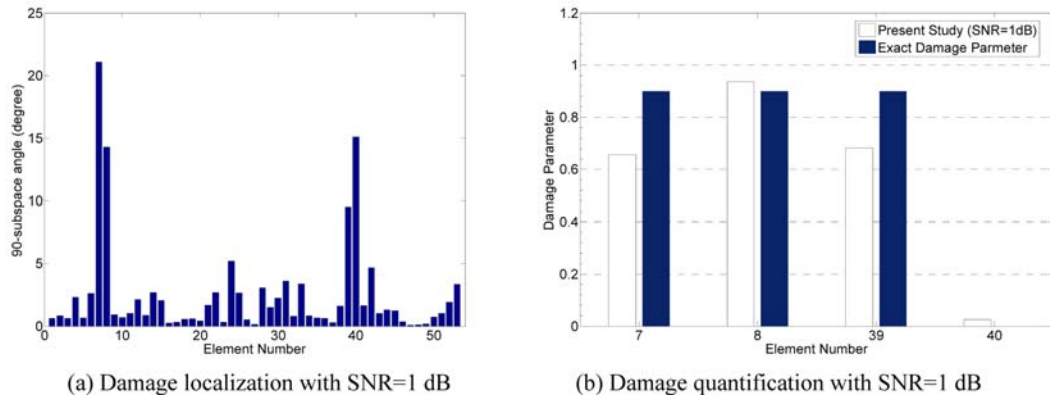
Fig. 11 Selection of damaged elements and quantification of damage extent; sensor noise (SNR = 1 dB) for damage scenario 2; NExT = 45 windows averaged = 8 sec data; First 5 mode shapes were used
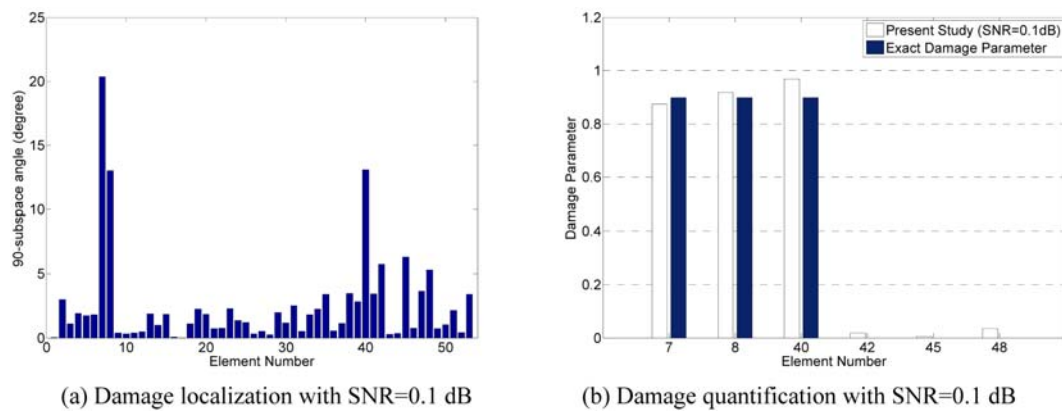

(a) Damage localization with SNR=0.1 dB (b) Damage quantification with SNR=0.1 dB

Fig. 12 Selection of damaged elements and quantification of damage extent; sensor noise (SNR = 0.1 dB) for damage scenario 2; NExT = 45 windows averaged = 8 sec data; First 5 mode shapes were used

which produced 360 windows when averaged using 8-second time signals. To observe the effects of the averaged number in NExT technique on final damage diagnosis results, we also tested using an increased number of points: 32,768 points for FFT, which produced 45 windows to be averaged. As summarized in Table 5, modal identification results are reliable up to 10 modes. It is notable that the number of average in NExT does not magnify noise effects on the damage diagnosis results. It is because the longer duration of time signals has effects nothing but increasing the frequency resolutions eventually resulting in longer impulse response.

6. Conclusions

In this paper, a new damage detection and quantification method has been demonstrated to perform a damage diagnosis of a truss bridge structure under ambient vibration. In practical aspects for monitoring civil infrastructure, the importance of using ambient vibration data has been well

recognized among researchers. NExT and ERA techniques are employed to identify modal properties using noisy ambient vibration data. Combining the parameter subset selection method with the steady state genetic algorithm, multiple damage locations could be located and quantified even under noisy ambient vibration environments. Highlights of observations and advantages from using the proposed method are presented as follows:

- The ERA analyses showed better performance with lightly damped structures than with highly damped structures.
- For five damage scenarios, noise effects on the identified modal properties in higher modes are more noticeable than those in lower modes.
- Damage effects on the modal properties identified by NExT/ERA appeared to be small.
- The subset selection method based on the sensitivity of the dynamic residual force can efficaciously detect multiple damage locations.
- The number of averaged windows in NExT technique has little effect on magnification of noise injected to ambient vibration data.
- The steady state genetic algorithm can further distinguish undamaged elements from damaged elements quantifying the level of the damage precisely.

According to the test results, the proposed method is shown to be very promising in structural health monitoring of real-life structures under ambient vibration. The method can be used either for damage diagnosis or model-based condition assessment.

In conclusion, the proposed damage diagnosis method has been demonstrated to quantitatively assess the damage in structures under ambient environments. For future research, the proposed method should be assessed with physical experiments or *in-situ* ambient measurements considering other types of ambient environmental effects such as temperature variations.

Acknowledgements

References

Amani, M.C., Riera, J.D. and Curadelli, R.O. (2007), "Identification of changes in the stiffness and damping matrices of linear structures through ambient vibrations", *Struct. Control Hlth. Monit.*, **14**(8), 1155-1169.

Bani-Hani, K.A., Zibdeh, H.S. and Hamdaoui, K. (2008), "Health monitoring of a historical monument in Jordan based on ambient vibration test", *Smart Struct. Syst.*, **4**(2), 195-208.

Beck, J.L., Vanik, M.W. and Katafygiotis, L.S. (1994), "Determination of model parameters from ambient vibration data for structural health monitoring", *Proceedings of 1st World Conference on Structural Control*, Pasadena, CA.

Bendat, J.S. and Piersol, A.G. (2000), *Random Data Analysis and Measurement Procedures*, John Wiley & Sons, Inc.

Bernal, D. (2002), "Load vectors for damage localization", *J. Eng. Mech.-ASCE*, **128**(1), 7-14.

Caicedo, J.M., Dyke, S.J. and Johnson, E.A. (2004), "Natural excitation technique and eigensystem realization algorithm for phase I of the IASC-ASCE benchmark problem: Simulated data", *J. Eng. Mech.-ASCE*, **130**(1), 49-60.

Caicedo, J.M. and Yun, G.J. (2011), "A novel evolutionary algorithm for identifying multiple alternative solutions

in model updating", *Struct. Control Hlth. Monit.*, **10**(5), 491-501.

Doebling, S.W., Farrar, C.R. and Prime, M.B. (1998), "A summary review of vibration-based damage identification methods", *Shock Vib. Dig.*, **30**(2), 91-105.

Duan, Z.D., Yan, G.R., Ou, J.P. and Spencer, B.F. (2007), "Damage detection in ambient vibration using proportional flexibility matrix with incomplete measured DOFs", *Struct. Control Hlth. Monit.*, **14**(2), 186-196.

Efroymson, M.A. (1960), *Multiple Regression Analysis*, John Wiley, New York.

Farrar, C.R. and James, G.H. (1997), "System identification from ambient vibration measurements on a bridge", *J. Sound Vib.*, **205**(1), 1-18.

Fox, R.L. and Kapoop, M.P. (1968), "Rates of change of eigenvalues and eigenvectors", *AIAA J.*, **6**(12), 2426-2429.

Friswell, M.I. and Penny, J.E.T. (1997), "The practical limits of damage detection and location using vibration data", *Proceedings 11th VPI&SU Symposium on Structural Dynamics and Control*, Blacksburg, VA.

Friswell, M.I., Penny, J.E.T. and Garvey, S.D. (1997), "Parameter subset selection in damage location", *Inverse Probl. Eng.*, **5**(3), 189-215.

Gao, Y. and Spencer, B.F. (2006), "Online damage diagnosis for civil infrastructure employing a flexibility-based approach", *Smart Mater. Struct.*, **15**(1), 9-19.

Gentile, C. and Gallino, N. (2008), "Condition assessment and dynamic system identification of a historic suspension footbridge", *Struct. Control Hlth. Monit.*, **15**(3), 369-388.

Gokdag, H. and Kopmaz, O. (2010), "A new structural damage detection index based on analyzing vibration modes by the wavelet transform", *Struct. Eng. Mech.*, **35**(2), 257-260.

Ho, B.L. and Kalman, R.E. (1965), "Effective construction of linear state-variable models from input/output data", *Proceedings of the 3rd Annual Allerton Conference in Circuit and System Theory.*

Ibrahim, S.R. and Mikulcik, E.C. (1977), "A method for direct identification of vibration parameters from the free response", *Shock Vib. Bull.*, **47**(4), 183-198.

James, G.H., Carne, T.G. and Lauffer, J.P. (1993), *The Natural Excitation Technique (NExT) for Modal Parameter Extraction From Operating Wind Turbines*, Sandia National Laboratory.

Juang, J.N. (1994), *Applied System Identification*, Prentice Hall, Inc.

Juang, J.N. and Pappa, R.S. (1985), "An eigensystem realization-algorithm for modal parameter-identification and model-reduction", *J. Guid. Control Dyn.*, **8**(5), 620-627.

Lallement, G. and Piranda, J. (1990). "Localization methods for parameter updating of finite element models in elastodynamics", *Proceedings of the 8th International Modal Analysis Conference*, Orlando, Florida.

Lee, L.S., Karbhari, V.M. and Sikorsky, C. (2007), "Structural health monitoring of CFRP strengthened bridge decks using ambient vibrations", *Struct Hlth. Monit*, **6**(3), 199-214.

Lynch, J.P., Sundararajan, A., Law, K.H., Kiremidjian, A.S. and Carryer, E. (2004), "Embedding damage detection algorithms in a wireless sensing unit for operational power efficiency", *Smart Mater. Struct.*, **13**(4), 800-810.

Nayeri, R.D., Masri, S.F. and Chassiakos, A.G. (2007), "Application of structural health monitoring techniques to track structural changes in a retrofitted building based on ambient vibration", *J. Eng. Mech.-ASCE*, **133**(12), 1311-1325.

Nayeri, R.D., Masri, S.F., Ghanem, R.G. and Nigbor, R.L. (2008), "A novel approach for the structural identification and monitoring of a full-scale 17-story building based on ambient vibration measurements", *Smart Mater. Struct.*, **17**(2), 025006 (19p).

Pappa, R.S. and Elliott, K.B. (1993), "Consistent-mode indicator for the eigensystem realization algorithm", *J. Guid. Control Dyn.*, **16**(5), 852-858.

Peeters, B., Maeck, J. and De Roeck, G. (2001), "Vibration-based damage detection in civil engineering: excitation sources and temperature effects", *Smart Mater. Struct.*, **10**(3), 518-527.

Ren, W.X. and Peng, X.L. (2005), "Baseline finite element modeling of a large span cable-stayed bridge through field ambient vibration tests", *Comput. Struct.*, **83**(8-9), 536-550.

Sim, S.H., Jang, S.A., Spencer, B.F. and Song, J. (2008), "Reliability-based evaluation of the performance of the damage locating vector method", *Probab. Eng. Mech.*, **23**(4), 489-495.

Siringoringo, D.M. and Fujino, Y. (2006), "Experimental study of laser Doppler vibrometer and ambient vibration for vibration-based damage detection", *Eng. Struct.*, **28**(13), 1803-1815.

Sohn, H., Farrar, C.R., Hemez, F.M., Shunk, D.D., Stinemates, D.W. and Nadler, B.D. (2003), *A Review of Structural Health Monitoring Literature: 1996-2001*, Los Alamos National Laboratory.

Song, W., Dyke, S.J., Yun, G.J. and Harmon, T.G. (2009), "Improved damage localization and quantification using subset selection", *J. Eng. Mech.-ASCE*, **135**(6), 548-560.

Stubbs, N., Park, S., Sikorsky, C. and Choi, S. (2000), "A global non-destructive damage assessment methodology for civil engineering structures", *Int. J. Syst. Sci.*, **31**(11), 1361-1373.

Syswerda, G. (1991), "A study of reproduction in generational and steady state genetic algorithms", *Proceedings of Foundations of Genetic Algorithms Conference*, Morgan Kaufmann.

Titurus, B., Friswell, M.I. and Starek, L. (2003), "Damage detection using generic elements: Part II. Damage detection", *Comput. Struct.*, **81**(24-25), 2287-2299.

Van Overschee, P. and De Moor, B.L. (1996), *Subspace Identification for Linear System: Theory-Implementation-Applications*, Springer.

Wong, K.Y. (2004), "Instrumentation and health monitoring of cable-supported bridges", *Struct. Control Hlth. Monit.*, **11**, 91-124.

Yun, G.J., Ogorzalek, K.A., Dyke, S.J. and Song, W. (2008), "A parameter subset selection method using residual force vector for detecting multiple damage location", *Struct. Control Hlth. Monit.,* DOI: 10.1002/stc.1284.

Yun, G.J., Ogorzalek, K.A., Dyke, S.J. and Song, W. (2008), "A structural damage detection method based on subset selection and evolutionary computation", *Proceedings of the 2008 Structures Congress*, Vancouver, Canada.